Lysophosphatidylcholine induces oxidative stress in human endothelial cells via NOX5 activation - implications in atherosclerosis

Josiane Fernandes da Silva[1], Juliano V Alves[1], Julio Neto[1], Rafael M Costa[1], Karla B Neves[2], Rheure Lopes[2], Livia Carmargo[2], Francisco Rios[2], Augusto Montezano[2], Rhian M Touyz[2], Rita C Tostes[1].

[1]Pharmacology Department, Ribeirao Preto Medical School, University of Sao Paulo (FMRP-USP)– USP, Brazil.

[2]Institute of Cardiovascular and Medical Sciences, BHF Glasgow Cardiovascular Centre, University of Glasgow, Glasgow, UK.

* Corresponding Author:

Rita C Tostes

Dept. of Pharmacology

Ribeirao Preto Medical School

University of Sao Paulo

Av Bandeirantes 3900

Ribeirao Preto - SP 14049-900

Brazil

Phone: +55 16 3315-4529 / 3315-3181

rtostes@usp.br

Abstract

Introduction: NOX5 belongs to the nicotinamide adenine dinucleotide phosphate (NADPH) oxidases (NOX) family, and its vascular expression and activity are up regulated in cardiovascular diseases, such as hypertension and atherosclerosis. Although NOXes are activated by many factors that contribute to formation and progression of atherosclerotic lesions, including lipids and oxidized low-density lipoprotein (oxLDL), mechanisms involved in NOX5 activation in atherosclerotic processes are still unclear. This study tested the hypothesis that lysophosphatidylcholine (LPC), a proatherogenic component of oxLDL, induces endothelial calcium influx, which drives NOX5-dependent reactive oxygen species (ROS) production, oxidative stress and endothelial cell dysfunction. **Methods:** Human aortic endothelial cells (HAEC) were stimulated with LPC (10^{-5} M, for different time points). Pharmacological inhibition of NOX5 (Melittin, 10^{-7} M) and NOX5 gene silencing (siRNA) were used to determine the role of NOX5-dependent ROS production in endothelial oxidative stress induced by LPC. ROS production was determined by lucigenin assay and electron paramagnetic spectroscopy (EPR), calcium transients by Fluo4 fluorimetry and NOX5 activity and protein expression by pharmacological assays and immunoblotting, respectively. **Results and Discussion**: LPC increased ROS generation in endothelial cells at both short (15 min) and long (4 h) stimulation times. LPC-induced ROS at both 15 min and 4 h was abrogated by a selective NOX5 inhibitor and by knockdown of NOX5 expression. NOX1/4 dual inhibition and selective NOX1 inhibition only decreased ROS generation at 4 h. LPC increased HAEC intracellular calcium, important for NOX5 activation, and this was blocked by nifedipine and thapsigargin. Bapta-AM and EGTA, selective

Ca^{2+} chelators, prevented LPC-induced ROS production. NOX5 knockdown decreased LPC-induced ICAM-1 mRNA expression and monocyte adhesion to endothelial cells.

Conclusion: These results suggest that NOX5, by mechanisms linked to increased intracellular calcium, is key to early LPC-induced endothelial oxidative stress and pro-inflammatory processes. Since these are important events in the formation and progression of atherosclerotic lesions, this study highlights an important role for NOX5 in atherosclerosis.

Introduction

Atherosclerosis remains a significant cause of morbidity and mortality worldwide, predisposing individuals to thrombosis, stroke, and other cardiovascular diseases (CVD) [1]. In the last decades, the advance in atherosclerosis knowledge has been remarkable. However, mechanisms involved in atherosclerotic plaque formation need further clarification in many aspects, including the role of NOX-induced oxidative stress [1].

The formation and progression of atherosclerotic lesions are directly related to oxidative stress in the vascular wall. Excessive reactive oxygen species (ROS) production is associated with endothelial dysfunction, lipids accumulation, apoptosis, inflammatory cytokines and monocyte recruitment [1, 2]. In all these processes, increased nicotinamide adenine dinucleotide phosphate (NADPH) oxidases (NOX) activity is key to increase superoxide anion (O_2^-) generation, which results in oxidative stress and more severe vascular lesions [1].

Four NOX isotypes are expressed in human endothelial cells, NOX1, NOX2, NOX4, and NOX5 [3]. These enzymes belong to a family of proteins that catalyze O_2 reduction to produce O_2^-, using NADPH as the electron donor ($NADPH + 2O_2 \rightarrow NADP^+ + H^+ + 2O_2^-$). NOX1, NOX2 and NOX4 require phox22 and other protein subunits, such as NOXOA1, phox67, and phox47 to function [3]. Unlike other NOX isoforms, NOX5 does not require modulatory subunits for its activation. The activity of this NOX isotype depends on gene expression, subcellular localization, post-translational changes, and cytoplasmic Ca^{2+} concentration ($[Ca^{2+}]i$). In endothelial cells, knockdown of NOX5 attenuates PCNA and VCAM expression induced by angiotensin II [4], suggesting that NOX5 plays a role in endothelial proliferation and monocyte

recruitment. Moreover, NOX5 expression is increased in patients with coronary artery diseases and associated with atherosclerosis severity [5]. However, mechanisms that induce NOX5 expression and activity in atherosclerosis remain to be elucidated.

Lysophosphatidylcholines (LPCs) are a group of bioactive lipids involved in the pathogenesis of atherosclerosis [6, 7]. LPC is a proatherogenic component of oxidized low-density lipoprotein (oxLDL) [8, 9] that activates pro-inflammatory and pro-oxidative cellular responses [10, 11, 12]. In humans, some LPC species are associated with atherosclerotic plaque [13, 14], and atheroma plaques from diabetic patients are significantly enriched with 2-arachidonoyl-lysophosphatidylcholine [15]. Furthermore, LPC induces endothelial cell activation through Ca^{2+}-dependent signaling [12] and mitochondrial ROS production [16]. However, it is not clear whether NOX5 contributes to LPC-induced endothelial oxidative stress.

Therefore, this study's premise is that LPC stimulates NOX5 activity, which contributes to oxidative stress and endothelial dysfunction associated with atherosclerotic processes.

Material and Methods

Cell culture

To assess whether NOX5 contributes to LPC-induced ROS production, primary cultured, low passage (p5-p7), aortic endothelial cells (HAEC, ATCC®, Middlesex, UK; PCS-100-011) were used. HAEC were cultured in endothelial cell growth medium (Promocell®) supplemented with penicillin/streptomycin (50 µg/mL) and endothelial cell growth medium supplement (10 mL, Promocell®). Before stimulation protocols, confluent cells were made quiescent by incubation for two hours (h) in low-serum medium (0.5% fetal bovine serum, FBS). For the mechanistic studies, drugs and their respective concentrations were as follows: Lysophosphatidylcholine (Sigma-Aldrich, cat. Number: L-4129, 10^{-5} M, [17]); Tiron (ROS scavenger, Sigma-Aldrich, cat number:172553, 10^{-4} M, [18]); GKT137831 (NOX1/4 inhibitor, Cayman chemical, 10^{-5} M, [19]); NoxA1ds (NOX1 inhibitor, Tocris, 10^{-5} M, [19]); Melittin (NOX5 inhibitor, 10^{-7} M, [20]); Nifedipine (L-type calcium channel blocker, Tocris, 10^{-8} M, [21]); Thapsigargin (SERCA ATPase inhibitor, Tocris, 10^{-7} M, [22]), Ionomycin (Calcium ionophore, Tocris, 10^{-6} M, [23]), Bapta-AM (membrane-permeant selective Ca^{2+} chelator, Invitrogen, 5 x 10^{-6} M, [24], EGTA (Ca^{2+} chelator, Sigma-Aldrich, 2 x 10^{-3} M, [25]). Cells were incubated with the inhibitors, in individual protocols, for 30 minutes (min) before the stimulation with LPC. The inhibitors were kept during the stimulation with LPC.

ROS measurement by Chemiluminescence assay

LPC-induced ROS generation was assessed by chemiluminescence with NADPH as the substrate and lucigenin as the electron acceptor [26].

Endothelial cells were stimulated with LPC (10^{-5} M) for various time intervals: 5 min, 15 min, 30 min, 1 h, 4 h, 8 h, and 24 h. The two highest ROS production stimulation times were chosen to study LPC's mechanisms leading to ROS generation. In some experiments, cells were pre-incubated for 30 min with inhibitors, as described above. After stimulation, cells were washed with PBS and harvested in 100 µL lysis buffer [$2x10^{-2}$ M KH_2PO_4; 10^{-3} M EGTA, and protease inhibitors: 1 µg/ml of aprotinin, 1 µg/ml of leupeptin, 1 µg/ml of pepstatin, and 10^{-3} M phenylmethylsulfonyl fluoride (PMSF)]). 50 µL of the sample were added to 175 µL assay buffer [$5x10^{-2}$ M KH_2PO_4, 10^{-3} M EGTA, $1.5x10^{-3}$ M sucrose, and $5x10^{-6}$ M lucigenin (98% purity, Sigma)]. Then, the first reading was performed and considered as basal reading. NADPH (98% purity, 10^{-4} M; Sigma) was added to each sample, and the luminescence signal was measured, for 30 cycles of 18 seconds each, in a luminometer (Lumistar Galaxy, BMG Lab Technologies, Germany). Basal and blank buffer readings were subtracted from the respective samples reading. Results are expressed as a percentage of control values (% of control) of the relative light units (RLU) per protein content, as measured by the BCA assay (Thermo Fisher, 23225).

Superoxide anion (O_2^-) quantification by Electron Paramagnetic Resonance (EPR) spectroscopy

The cell-permeable spin-trapping probe, CMH (1-hydroxy-3-methoxycarbonyl-2,2,5,5-tetramethylpyrrolidine; Enzo life science, UK; cat. ALX430117), was used to detect intracellular superoxide anion in HAEC by EPR spectroscopy [27, 28]. After each experimental condition, cells were washed with sterile PBS and incubated in Krebs/Hepes buffer (pH= 7.35) containing 0.5 mM CMH, 5 µM

DETC, 25 µM deferoxamine for 30 min in a CO_2 incubator at 37°C. The solution was removed, and 100 μL of Krebs/Hepes buffer without CMH was added and then, cells were gently and quickly scraped. Approximately 50 μL were transferred into a capillary glass tube (Noxygen Science Transfer &Diagnostics) and placed inside the E-scan spectrometer's cavity for reading. The remaining sample volume was used for total protein determination by the BCA method (Pierce™ BCA Protein Assay Kit, Thermo Fisher Scientific, cat. 23225). The results are expressed as a percentage of the control condition, spectrum amplitude value (in arbitrary units) per protein concentration. Acquisition spectrometer (Bruker® Biospin Corp.) parameters were microwave power 21.98mV; microwave frequency 9.463GHz; number of scans 30; sweep width 50G; modulation amplitude 2G; conversion time, 656 ms; time constant, 656 ms; resolution, 512 points and receiver gain $1x10^5$. The sample temperature was kept at 21°C by the Temperature & Gas Controller unit, connected to the spectrometer. Spectra were analyzed by using Win EPR software, supplied by Bruker Corp.

Immunoblotting

Quiescent HAECs were stimulated with LPC 10^{-5} M for 15 min or 4 h, in the presence of vehicle or different inhibitors at 37°C. After stimulation, cells were quickly washed in ice-cold PBS, and protein extraction was performed in lysis buffer [50 mmol/L Tris-HCl (pH 7.4) containing 1% Nonited P-40, 0.5% sodium deoxycholate, 150 mmol/L NaCl, 1 mmol/L EDTA, 0.1% sodium dodecyl sulfate (SDS), 1 mmol/L phenylmethylsulfonyl fluoride (PMSF), 1 µg/mL pepstatin A, 1 µg/mL leupeptin and 1 µg/mL aprotinin]. Then, the lysate was

sonicated and cleared by centrifugation at 10,000 rpm for 10 min. Protein concentration was assessed by the BCA method (Pierce™ BCA Protein Assay Kit, Thermo Fisher Scientific, cat. 23225). 30 ug protein were separated by electrophoresis on 10% SDS polyacrylamide gel and transferred to a nitrocellulose membrane. Membranes were blocked with Tris-buffered solution (TBS) containing 5% skim milk and 0.01 % Tween for 1 h at room temperature. Then, membranes were incubated with specific primaries antibodies overnight at 4°C, and secondaries antibodies for 1 hour at room temperature. Primary and secondary antibodies used in Western blot assays were as follows: rabbit anti-NOX5 (Abcam / ab191010 /1:1000); β-actin (Cell Signaling Technology / # 4967 / 1:3000); peroxidase (HRP)-conjugated-anti-Rabbit IgG (Sigma / A0545 / 1:7500). Immunocomplexes were detected by chemiluminescence reaction (Luminata Forte HRP Substrate; Millipore, USA), and densitometric analysis was performed with ImageQuant 1.3 software. Protein expression levels were normalized to the internal housekeeping protein (β-actin).

Quantitative PCR (qPCR)

mRNA expression of NADPH oxidase 5 (NOX5), intercellular adhesion molecule 1 (ICAM1) and glyceraldehyde 3-phosphate dehydrogenase (GAPDH) was quantified by qPCR in non-stimulated endothelial cells or LPC-stimulated cells for 4 h or NOX5-silenced LPC-stimulated cells. Briefly, TRIzol® Reagent (Invitrogen) was used to extract total RNA from cells. RNA was treated with RNase-free DNAse I, and 2 µg of RNA was used in reverse transcriptase reactions, following the manufacturer's instruction (High capacity cDNA, Applied Biosystems #4368813). TaqMan Fast Advanced Master Mix (Applied

Biosystems, # 4444557) was used to perform real-time PCR amplification. The relative mRNA expression (target gene/ housekeeping gene) was calculated by the $2^{-\Delta\Delta CT}$ method. The assay primers used are as follows: h_NOX5 (Hs00225846_m1); h_ICAM-1, (Hs00164932_m1); h_GAPDH (Hs02786624_g1), from Thermo Fisher Scientific.

Calcium influx measurement

Calcium signal was assessed by dye Fluo-4 fluorescence (Invitrogen, F14201). After a 45-minute incubation period with the inhibitors, cells were quickly washed in Phosphate-buffered saline (PBS) and DMEM solution, without phenol and with Fluo-4 AM (2 µM), was added, for 30 min at 37º C, to load the cells. Following incubation, cells were washed and incubated with the medium for 20 min at 37ºC. Fluorescence-based measurements of Ca^{2+} were performed using a fluorimeter plate reader (FlexStation 3 system, Molecular Devices, San Jose, CA, USA). The software was set to acquire five basal readings with an interval of 30 seconds (s). LPC solution (10^{-5} M, final concentration) was added to cells and readings were recorded every 90 s, for 20 min. The excitation/emission wavelengths for the Fluo-4 signal recordings were 495 / 505 nm, respectively, and values were normalized to the basal value recording. LPC-induced extracellular calcium influx was evaluated in cells pre-incubated with nifedipine (L-type calcium channel blocker, Tocris, 10^{-8} M). Additionally, the role of intracellular endoplasmic reticulum calcium stocks in the LPC effects was estimated in cells pretreated with thapsigargin (SERCA ATPase inhibitor, Tocris, 10^{-7} M). Cells treated with ionomycin (Calcium ionophore, Tocris, 10^{-6} M) were used as a positive control. The results were

expressed as intensity of the signal (F)/ basal signal (F0) mean (RFU, relative fluorescence units) or area under the curve (AUC) of the fluorescence signal.

NOX5 Silencing

NOX5 downregulation was performed in HAEC using NOX5 siRNA (ID s35770, Silencer® Select siRNA, Thermo Fischer Scientific) complexed with Lipofectamine™ RNAiMAX (Thermo Fischer Scientific) as transfection reagent in Opti-MEM (GIBCO™) without serum or antibiotics for 24 h. A non-targeting negative control siRNA with the same chemical modifications (Silencer® Select Negative Control No. 1 siRNA, Invitrogen) was used as control siRNA. NOX5 protein expression was performed to confirm downregulation of NOX5 expression.

Monocyte attachment assay

To evaluate whether NOX5 contributes to monocytes adhesion on endothelial cells, NOX5-silenced endothelial cells were stimulated with LPC and exposed to fluorescence-labeled monocytes. The adhered cells were estimated by the fluorescence signal [29, 30]. Briefly, HAEC were cultured in 24-well plates, and NOX5 silencing was performed as described above. Then, the cells were stimulated with LPC 10^{-5} M for 4 h. Monocytes obtained from the American Type Culture Collection (THP-1) were cultured in RPMI medium supplemented with penicillin/streptomycin and 10% FBS. THP-1 were washed and incubated in saline solution containing 0.1% bovine serum albumin and 10^{-6} M of CellTrace CFSE Cell Proliferation (Life Technologies), a fluorescent probe, for 20 min at 37°C. After the stimulation period, HAEC were washed twice in

PBS and incubated with labeled monocytes ($2x10^5$ cells/mL) for 30 min at 37°C in 5% CO_2 to allow adhesion. At the end of this step, non-adherent monocytes were removed by gently washing with PBS, and the cells were de-attached with trypsin and transferred to an opaque plate. Images from the labeled monocytes were captured in a fluorescence microscope (Leica DMI inverted microscope) and the fluorescence signal was acquired with a fluorimeter plate reader (FlexStation 3 system, Molecular Devices, San Jose, CA, USA). The fluorescence signal estimated the number of adherent monocytes.

Statistical analysis

Statistical analysis of data was performed using GraphPad Prism 8.0 (GraphPad Software, San Diego, CA). Data are represented as mean ± standard error of the mean (SEM). Differences among the groups were evaluated using Student's t-test or one-way ANOVA followed by Dunnett's or Tukey post-test, when appropriated. $p < 0.05$ was considered statistically significant.

Results

LPC induces ROS production in HAEC cells

To determine ROS generation induced by LPC, HAEC were stimulated with LPC (10^{-5} M) for various times: 5 min, 15 min, 30 min, 1 h, 4 h, 8 h, and 24 h (figure 1). LPC induced ROS generation in endothelial cells (HAEC) in a time-dependent manner (figure 1). ROS levels increased after 15 min and increased up to 4 h after stimulation with LPC (10^{-5} M). After 4 h, ROS levels returned to the basal condition (figure 1C). In the subsequent experimental protocols, LPC-induced ROS generation was assessed at two time points: 15 min and 4 h.

LPC-induced ROS production is prevented by NOX5 pharmacological inhibition and by NOX5 siRNA silencing

To determine whether LPC influences endothelial cell ROS generation through NOX-dependent processes, cells were exposed to different NOX isoform inhibitors. First, endothelial cells were pre-incubated with GKT137831 10^{-5} M, a NOX1/4 dual inhibitor. GKT137831 did not reduce LPC-induced ROS generation at 15 min (figure 2A) but prevented ROS production at 4 h of LPC stimulation (figure 2B), suggesting that NOX 1 and 4 do not participate in the early stages of LPC-induced ROS generation. ROS generation in figure 2 was determined by Lucigenin assay. Similar results were observed using EPR spectroscopy (Supplementary figure 1).

Moreover, NOX 1 inhibition (noxa1ds 10^{-5} M) attenuated ROS production induced by LPC stimulation at 4 h (Supplementary figure 1D), but not at 15 min, supporting that NOX1 participates in ROS production induced by LPC at later-times.

Unlike GKT137831 and noxa1ds, Melittin (10^{-7} M), a NOX5 pharmacological inhibitor, blocked LPC-induced ROS generation at both early and late stimulation time points (figure 3). ROS generation was determined both by lucigenin assay (figures 3A and 3B) and EPR spectroscopy (figures 3C and 3D).

Supporting data from the pharmacological assays, silencing of NOX5 expression (siRNA) attenuated LPC-induced ROS production in HAEC cells (figure 4).

LPC stimulates calcium influx

An important mechanism for NOX5 activation is binding to intracellular calcium. To determine whether LPC increases intracellular calcium concentration at early time points of stimulation and whether this is linked to NOX5-dependent ROS production, calcium transients were measured using the Fluo-4 probe. LPC stimulation induced a significant increase in endothelial cell Fluo4 signal (figure 5A), which was blocked by nifedipine and thapsigargin (figure 5B). Moreover, EGTA, an extracellular Ca^{+2} chelator, and Bapta-AM, an intracellular Ca^{+2} chelator, abrogated ROS generation induced by LPC stimulation at 15 min (figure 5C).

NOX5 knockdown attenuates LPC-induced inflammatory processes in endothelial cells

LPC increased monocyte adhesion to endothelial cells and increased ICAM-1 expression. NOX5 knockdown decreased LPC-induced monocyte adhesion to endothelial cells (figures 6A and 6B). ICAM-1 mRNA expression

was also attenuated in NOX5-silenced endothelial cells stimulated with LPC (figure 6C).

Discussion

Oxidative stress is a critical player in endothelial dysfunction associated with cardiovascular diseases. NOX enzymes play a major role in the upregulated ROS production in atherosclerotic processes. However, the mechanisms involved in NOXes activation are not entirely understood. Here, we show that (1) LPC induces ROS production dependent on different NOX isoforms at different time points; ROS production induced by LPC involves NOX1/4 and NOX5 isotypes at late time points while NOX5 is important at early time points; (2) LPC increases intracellular Ca^{2+} concentration and induces a pro-inflammatory response in endothelial cells; (3) Calcium chelators prevent LPC-induced endothelial ROS production; (4) NOX5 pharmacological inhibition as well as NOX5 knockdown attenuates LPC-induced ROS generation and endothelial cell activation.

LPC is an abundant component of oxidized low-density lipoprotein (oxLDL) [30-33]. LPC activates apoptotic signaling [34, 35], induces vascular dysfunction [32], promotes inflammatory cells infiltration of vascular walls [36], and induces innate immune trans-differentiation of endothelial cells [12]. Upregulated ROS production contributes to the activation of signaling pathways that result in endothelial injury. LPC-induced ROS generation has been associated with NOX activation in HUVEC [37], leading to decrease NO bioavailability and caspase-3 activation. However, the NOX isotype that participates in this process was not identified.

LPC-induced ROS generation seems to be endothelial cell type-dependent since Tsai et al. failed to observe this effect in cerebral bEND.3 endothelial cells [34]. Here, we found that LPC (10^{-5} M) induces ROS

production in a time-dependent manner in aortic endothelial cells (HAEC). This pattern could be related to substrate availability for enzymatic ROS production, such as the NADPH oxidase-dependent ROS production.

Guzik et al. [5] observed that arterial NOX5 protein expression is increased in patients with coronary artery disease, contributing to increased ROS production. As hyperlipidemia plays an important role in atherosclerosis-related endothelial dysfunction, we used pharmacological inhibitors with differential selectivity for the NOX isotypes to determine which NOX isotypes contribute to LPC effect. In addition, different methodologies were used to detect and confirm ROS production by LPC and to investigate the participation of NOX5 in LPC-induced endothelial ROS production. Lucigenin and electron paramagnetic spectroscopy showed NOX5-dependent ROS generation at early time points for LPC stimulation. NOX5 knockdown decreased LPC-induced ROS production, supporting data obtained in pharmacological assays. Moreover, the continuous presence of LPC activated other NOX isotypes that, along with NOX5, sustain ROS production, as demonstrated by decreased ROS production in the presence of NOX1/4 dual inhibitor or selective NOX1 and NOX5 inhibitors. These findings suggest that LPC induces NOX5 activity and NOX5 inhibition attenuates or delays oxidative stress in hyperlipidemia conditions, such as atherosclerosis.

Activation of different NOX isotypes under prolonged LPC stimulus may be associated with ROS-induced ROS release [36, 37]. Sustained ROS production can overwhelm the cellular ROS quenching capacity, leading to redox unbalance, and oxidation of essential mitochondrial components (as revised by Zorov DB. *et al* [38]) or of enzymes that modulate NOXes activity,

such as Src-family kinases [39] and others, like tyrosine phosphatases, whose activity is inhibited by oxidation [40]. Inhibition of tyrosine phosphatase can also increase ROS generation by disturbing tyrosine kinase signaling and organelles function [19, 41]. Therefore, modulation of NOX5-dependent ROS generation, as observed in the early stages of LPC stimulation, may prevent irreversibly cellular damage related to ROS overproduction.

LPC incubation for longer period times (for 4 hours) did not change NOX5 expression in endothelial cells (data not shown). However, LPC increased intracellular Ca^{2+} concentration at time points where increased ROS production was observed. Unlike other NOX isotypes, NOX5 activity relies on Ca^{2+} influx [3, 5]. Despite of unchanged NOX5 protein expression, NOX5 activity was increased. Additionally, Ca^{2+} mobilization induced by LPC seems to depend on both intra- and extracellular calcium stocks, since nifedipine, a membrane calcium channel blocker, and thapsigargin, which perturbs and reduces endoplasmic reticulum Ca^{2+} stock, prevented LPC-induced increased intracellular Ca^{+2} concentrations. The calcium machinery is extremely complex [42] and LPC perturbation of endothelial Ca^{2+} homeostasis demonstrates that it may trigger many cellular mechanisms [12, 43], including activation of NOX5, and, consequently, ROS production.

Finally, LPC has been shown to activate inflammatory signaling pathways in endothelial cells [12], inducing cytokine production [44] and upregulating adhesion molecules expression [45]. Here, we observed that NOX5 knockdown attenuated LPC-induced ICAM-1 mRNA expression as well as monocyte adhesion, important events in atherosclerosis development and progression.

Together, these results suggest that control of NOX5 in pathological conditions may improve endothelial function and attenuate inflammatory responses to LPC.

In conclusion, our results demonstrate that NOX5-dependent ROS production is essential to LPC-induced oxidative stress and inflammatory response in endothelial cells. Moreover, our data suggest that NOX5 represents an important target to prevent endothelial cells activation and atherosclerosis-associated oxidative and inflammatory processes.

Legends to Figures

Figure 1 - LPC-induced ROS production in HAEC. (A) ROS production after short-time stimulations (5 min – 1 h). (B) ROS production after long-time stimulations (4 h – 24 h). (C) Line graphic showing the profile of LPC-induced ROS production, assessed by lucigenin assay. Data represent the mean ± SEM of n=5-8 experiments. One-way ANOVA followed by Tukey's multiple comparisons test. * $p<0.05$.

Figure 2 - Role of NOX1 and NOX4 in LPC-induced ROS generation in endothelial cells. LPC stimulation for 15 min (A, C) and 4 h (B, D) in the presence of vehicle or GKT137831 (10^{-5} M, NOX1/4 inhibitor) or noxa1ds (10^{-5} M, NOX1 inhibitor). ROS generation was determined by Lucigenin assay. Data represent the mean ± SEM. One-way ANOVA followed by Tukey's multiple comparisons test. *$p<0.05$ and, ns= not significant.

Figure 3 - Role of NOX5 in LPC-induced ROS generation in endothelial cells. ROS generation was measured by Lucigenin assay (A, B) and EPR spectroscopy (C, D). LPC stimulation for 15 min (A, C) and 4 h (B, D) in the presence of vehicle or Melittin (10^{-7} M, NOX5 inhibitor). Data represent the mean ± SEM of n= 4-10 experiments. One-way ANOVA followed by Tukey's multiple comparisons test. * $p<0.05$.

Figure 4 – NOX5 knockdown abrogates LPC-induced ROS generation. ROS generation was measured by Lucigenin assay (A) in cells stimulated with LPC (10^{-5} M) for 15 min. Endothelial NOX5 protein expression in control cells (control), cells with negative control siRNA (mismatch) or siRNA for NOX5 (B). Data represent the mean ± SEM of n= 4-6 experiments. Two-way (A) or one-way (B) ANOVA followed by Tukey's multiple comparisons test. * $p<0.05$ and, ns = not significant.

Figure 5 – LPC-induced calcium mobilization in endothelial cells. Relative Fluo4 fluorescence signal during 30 min of LPC (10^{-5} M) stimulation (A). Area under the curve (AUC) from data depicted in A (B). ROS generation was measured by Lucigenin assay in cells stimulated with LPC (10^{-5} M) for 15 min in the presence of Bapta-AM (10^{-6} M), EGTA (2×10^{-3} M) or Tiron (10^{-4} M) (C). Data represent the mean ± SEM of n= 5-7 experiments. One-way ANOVA followed by Tukey's multiple comparisons test. * $p<0.05$.

Figure 6 – NOX5 knockdown attenuates endothelial cell activation. Photomicrography depicting labeled monocytes (CFSE probe, green) on LPC- or vehicle-stimulated control endothelial cells (vehicle, lipofectamine), endothelial cells submitted to NOX5 silencing (siRNA) or negative control siRNA sequence (mismatch) (A). Fluorescence signals from labeled monocytes in A (B). ICAM-1 mRNA expression (C). Data represent the mean ± SEM of n= 5-8 experiments. Two-way ANOVA followed by Tukey's multiple comparisons test. *$p<0.05$.

459 **Figure 1**

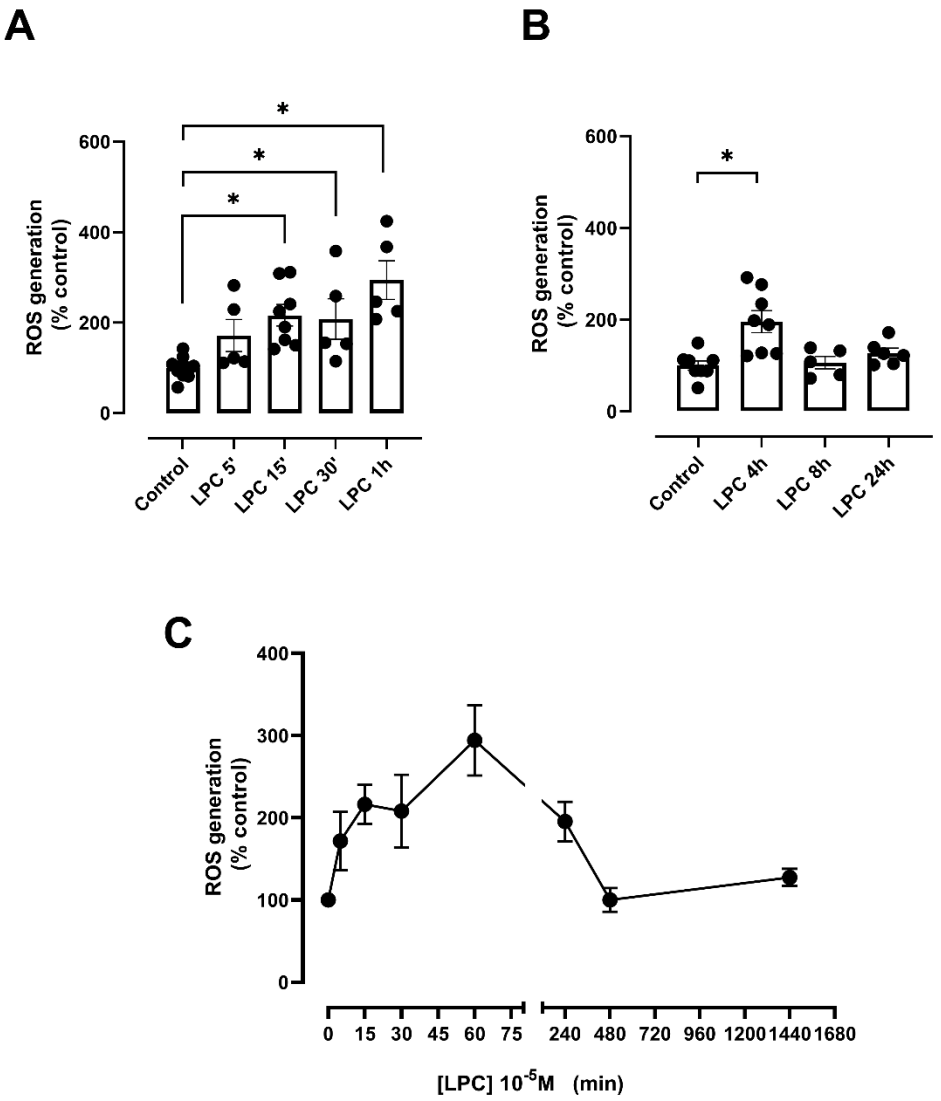

460

461

462 **Figure 2**

463

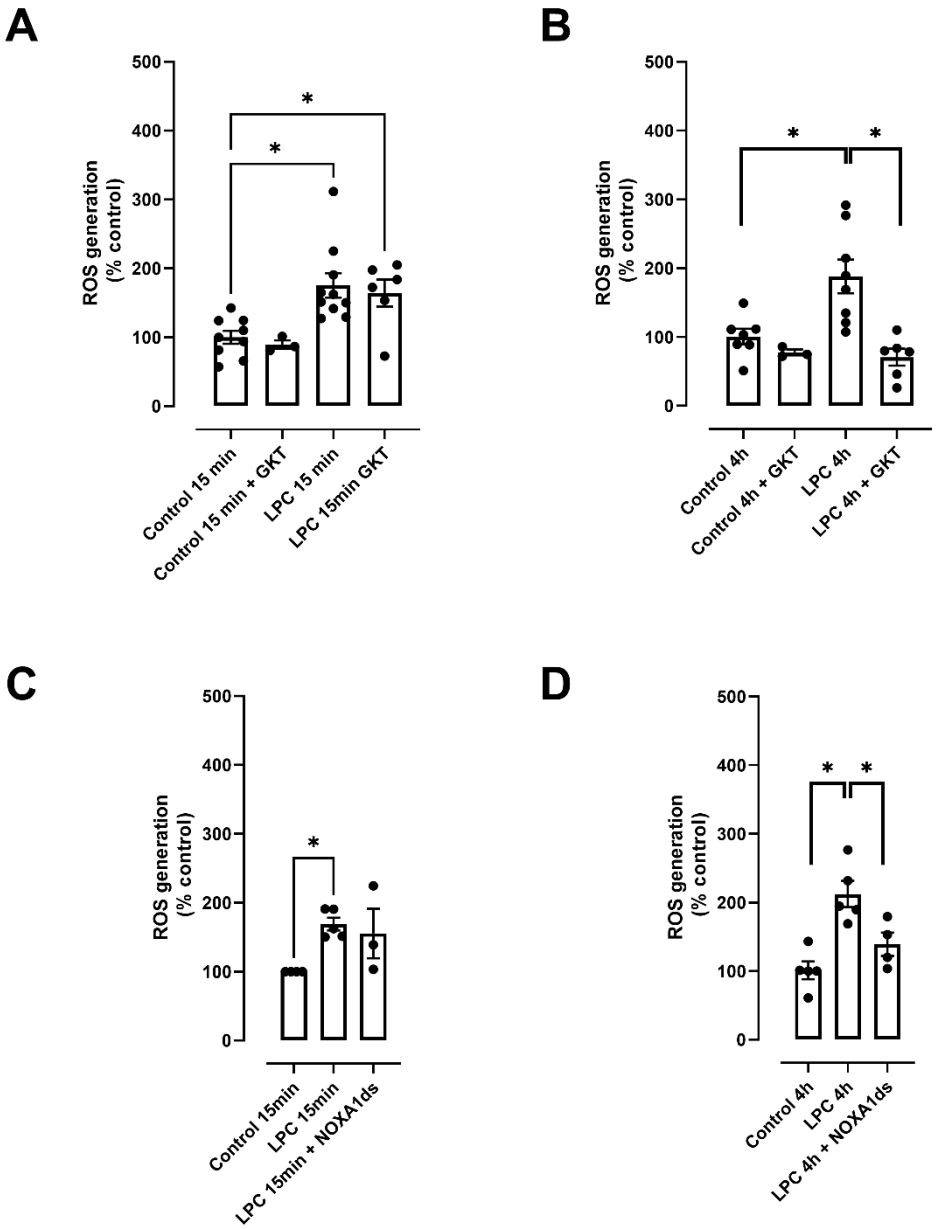

464

465

Figure 3

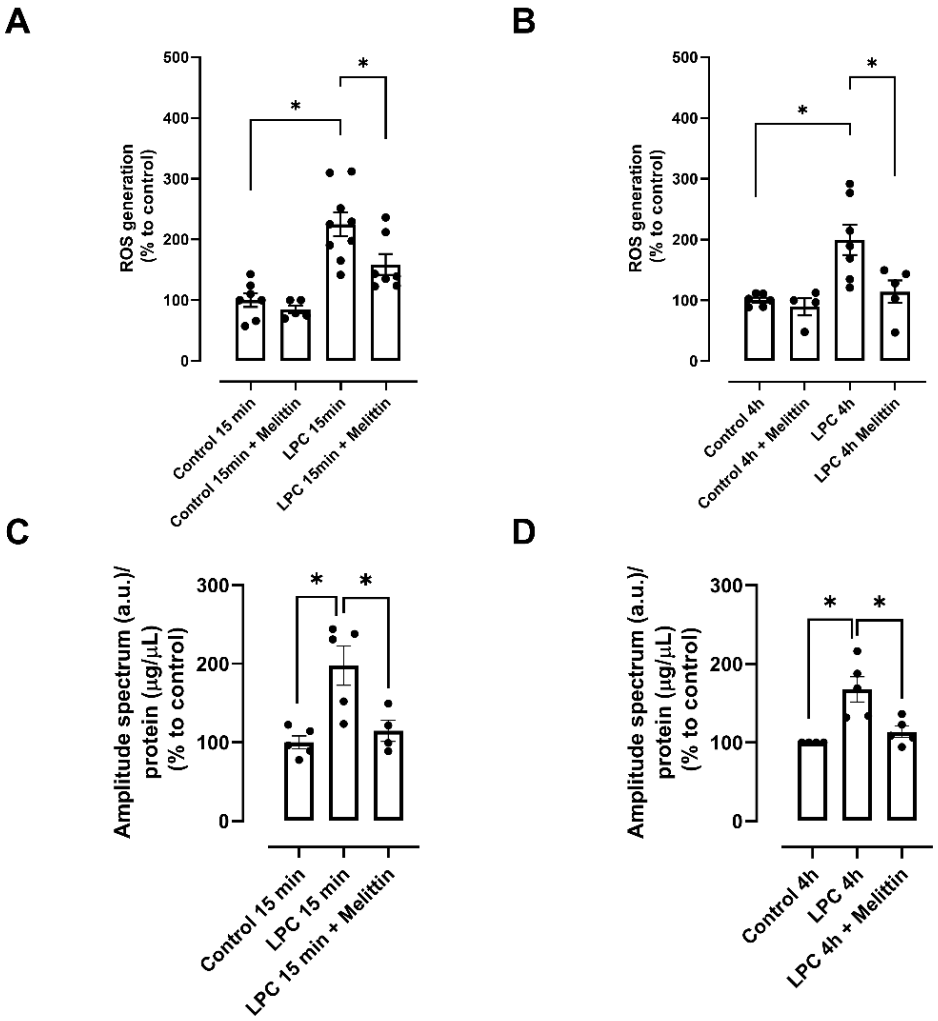
A
ROS generation (% to control)
500
400
300
200
100
0
*
*
Control 15 min
Control 15min + Melittin
LPC 15min
LPC 15min + Melittin
B
ROS generation (% to control)
500
400
300
200
100
0
*
*
Control 4h
Control 4h + Melittin
LPC 4h
LPC 4h Melittin
C
Amplitude spectrum (a.u.)/ protein (µg/µL) (% to control)
300
200
100
0
*
*
Control 15 min
LPC 15 min
LPC 15 min + Melittin
D
Amplitude spectrum (a.u.)/ protein (µg/µL) (% to control)
300
200
100
0
*
*
Control 4h
LPC 4h
LPC 4h + Melittin

Figure 4.

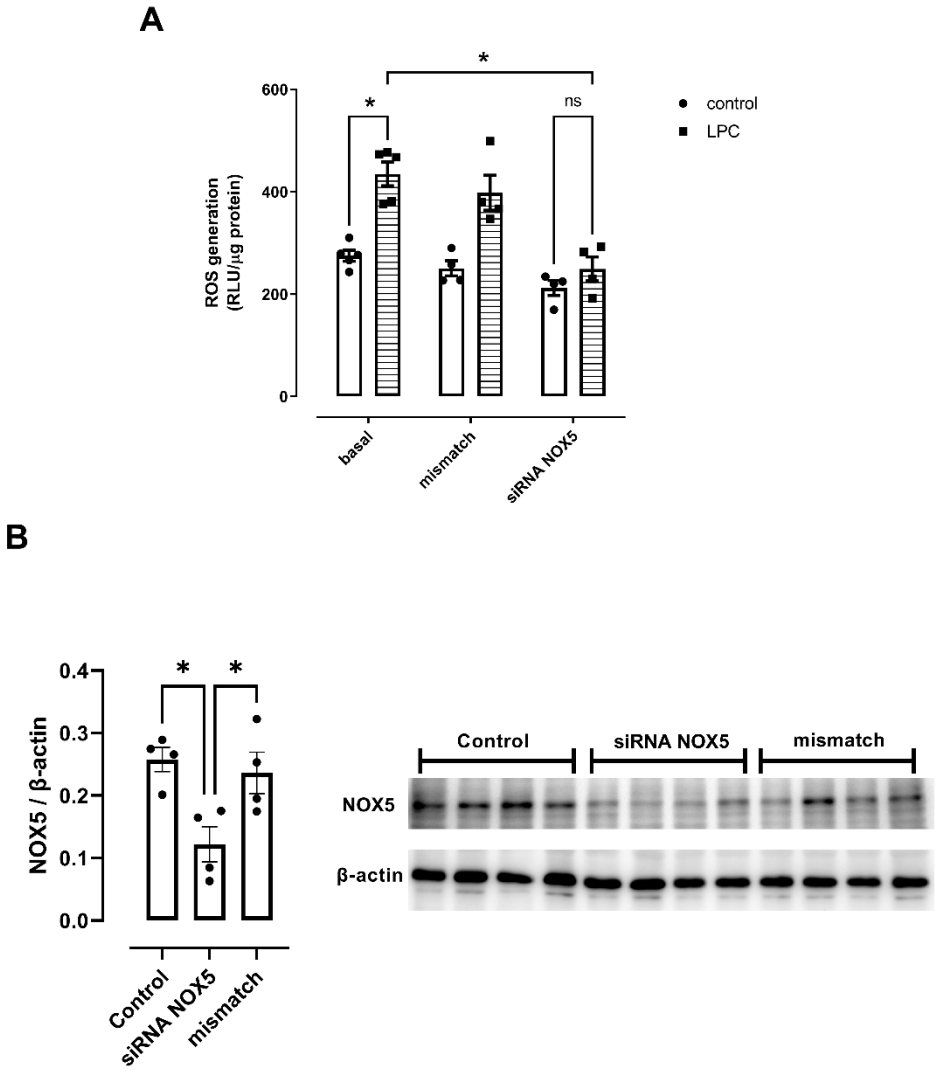
A
ROS generation (RLU/µg protein)
600
400
200
0
*
*
ns
control
LPC
basal
mismatch
siRNA NOX5
B
NOX5 / β-actin
0.4
0.3
0.2
0.1
0.0
*
*
Control
siRNA NOX5
mismatch
Control
siRNA NOX5
mismatch
NOX5
β-actin

Figure 5

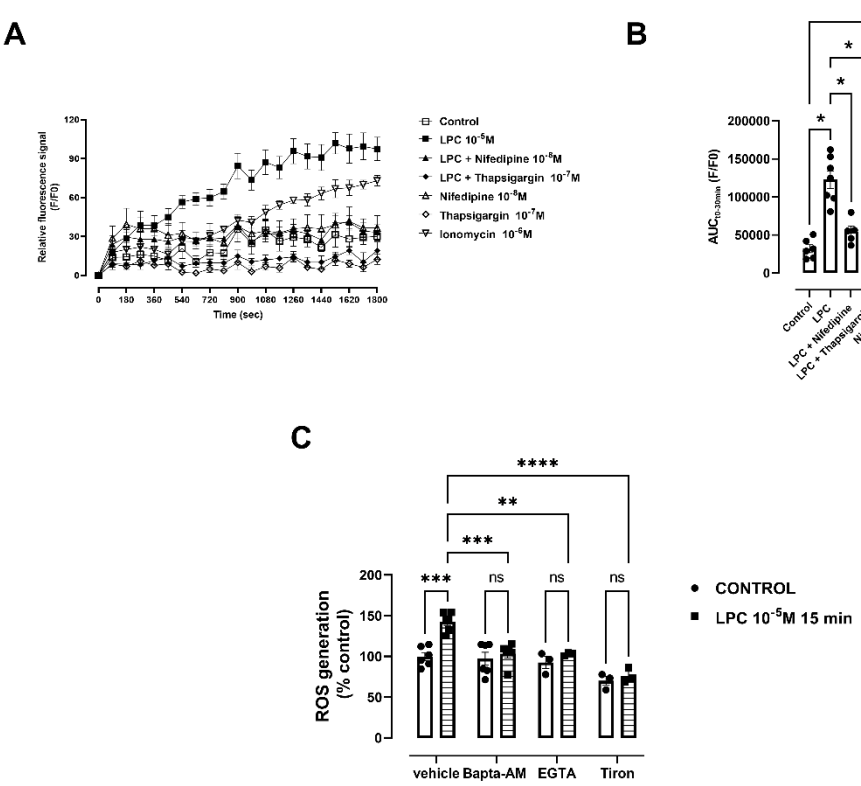
A
Relative fluorescence signal (F/F0)
Time (sec)
Control
LPC 10-5M
LPC + Nifedipine 10-5M
LPC + Thapsigargin 10-7M
Nifedipine 10-5M
Thapsigargin 10-7M
Ionomycin 10-6M
B
AUC0-30min (F/F0)
Control
LPC
LPC + Nifedipine
LPC + Thapsigargin
Nifedipine
Thapsigargin
Ionomycin
C
ROS generation (% control)
vehicle
Bapta-AM
EGTA
Tiron
CONTROL
LPC 10-5M 15 min

481 **Figure 6.**

482

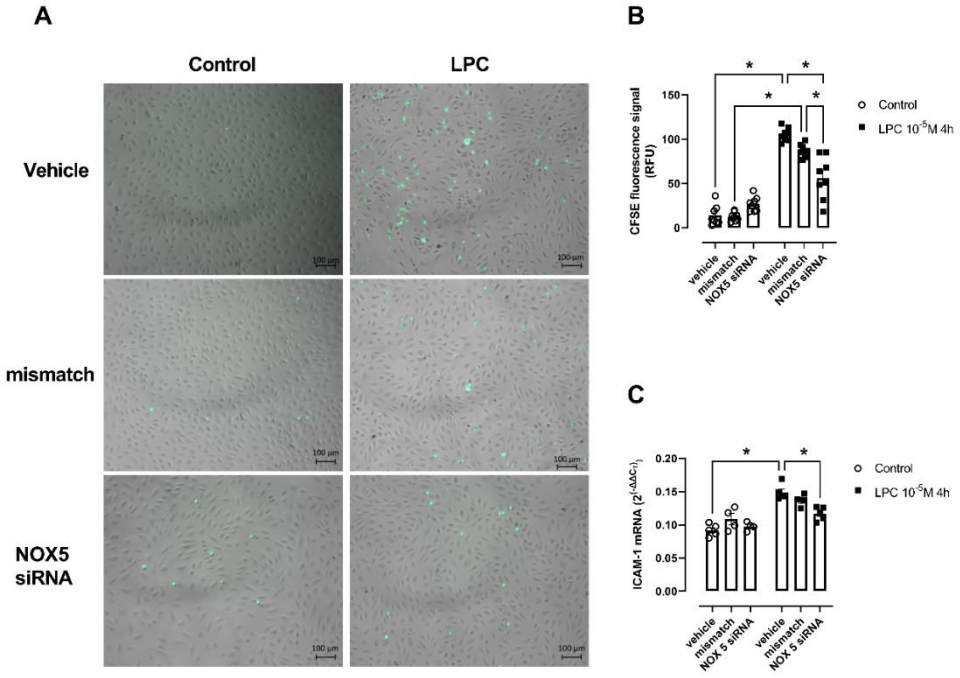

483

484

Acknowledgments

This work was supported by grants from Fundação de Amparo à Pesquisa do Estado de São Paulo (FAPESP-CRID 2013/08216-2; 2016/16207-1 to JFS), Coordenação de Aperfeiçoamento de Pessoal de Nível Superior (CAPES) and Conselho Nacional de Desenvolvimento Científico e Tecnológico (CNPq), Brazil, to RCT.

Conflict of Interest

All authors declare no conflict of interest.

Author Contributions

All authors participated in the design of the study

JFS, JVA, JN, RMC - performed the experiments

RCT and RMT contributed with reagents or analytical tools

JFS - performed the data analysis

JFS and RCT wrote the paper

All authors discussed and critically reviewed the material

Supplementary Material

Supplementary Material is available on Arteriosclerosis, Thrombosis, and Vascular Biology website. (ATVB 6.6) AHA

References

[1] - Yang X, Li Y, Li Y, et al. Oxidative Stress-Mediated Atherosclerosis: Mechanisms and Therapies. Front Physiol. 2017; 8:600. Published 2017 Aug 23. doi:10.3389/fphys.2017.00600.

[2] - Gimbrone MA Jr, García-Cardeña G. Endothelial Cell Dysfunction and the Pathobiology of Atherosclerosis. Circ Res. 2016;118(4):620-636. doi:10.1161/CIRCRESAHA.115.306301.

[3] - Touyz RM, Anagnostopoulou A, Rios F, Montezano AC, Camargo LL. NOX5: Molecular biology and pathophysiology. Exp Physiol. 2019;104(5):605-616. doi:10.1113/EP086204.

[4] – Montezano AC, Burger D, Paravicini TM, et al. Nicotinamide adenine dinucleotide phosphate reduced oxidase 5 (Nox5) regulation by angiotensin II and endothelin-1 is mediated via calcium/calmodulin-dependent, rac-1-independent pathways in human endothelial cells. Circ Res. 2010;106(8):1363-1373. doi:10.1161/CIRCRESAHA.109.216036.

[5] - Guzik TJ, Chen W, Gongora MC, et al. Calcium-dependent NOX5 nicotinamide adenine dinucleotide phosphate oxidase contributes to vascular oxidative stress in human coronary artery disease. J Am Coll Cardiol. 2008;52(22):1803-1809. doi:10.1016/j.jacc.2008.07.063.

[6] - Law SH, Chan ML, Marathe GK, Parveen F, Chen CH, Ke LY. An Updated Review of Lysophosphatidylcholine Metabolism in Human Diseases. *Int J Mol Sci*. 2019;20(5):1149. Published 2019 Mar 6. doi:10.3390/ijms20051149.

[7] - Li YF, Li RS, Samuel SB, et al. Lysophospholipids and their G protein-coupled receptors in atherosclerosis. Front Biosci (Landmark Ed). 2016;21(1):70-88. doi:10.2741/4377.

[8] - Chen L, Liang B, Froese DE, et al. Oxidative modification of low density lipoprotein in normal and hyperlipidemic patients: effect of lysophosphatidylcholine composition on vascular relaxation. J Lipid Res. 1997;38(3):546-553.

[9] - Zakiev ER, Sukhorukov VN, Melnichenko AA, Sobenin IA, Ivanova EA, Orekhov AN. Lipid composition of circulating multiple-modified low density lipoprotein. *Lipids Health Dis*. 2016;15(1):134. Published 2016 Aug 24. doi:10.1186/s12944-016-0308-2.

[10] - Kume N, Cybulsky MI, Gimbrone MA Jr. Lysophosphatidylcholine, a component of atherogenic lipoproteins, induces mononuclear leukocyte adhesion molecules in cultured human and rabbit arterial endothelial cells. *J Clin Invest*. 1992;90(3):1138-1144. doi:10.1172/JCI115932.

[11] - Han MS, Lim YM, Quan W, et al. Lysophosphatidylcholine as an effector of fatty acid-induced insulin resistance. J Lipid Res. 2011;52(6):1234-1246. doi:10.1194/jlr.M014787.

[12] - Li X, Wang L, Fang P, et al. Lysophospholipids induce innate immune transdifferentiation of endothelial cells, resulting in prolonged endothelial activation. J Biol Chem. 2018;293(28):11033-11045. doi:10.1074/jbc.RA118.002752.

[13] - Diehl P, Nienaber F, Zaldivia MTK, et al. lysophosphatidylcholine is a Major Component of Platelet Microvesicles Promoting Platelet Activation and Reporting Atherosclerotic Plaque Instability. *Thromb Haemost*. 2019;119(8):1295-1310. doi:10.1055/s-0039-1683409.

[14] - Meikle PJ, Wong G, Tsorotes D, et al. Plasma lipidomic analysis of stable and unstable coronary artery disease. Arterioscler Thromb Vasc Biol. 2011;31(11):2723-2732. doi:10.1161/ATVBAHA.111.234096

[15] - Ménégaut L, Masson D, Abello N, et al. Specific enrichment of 2-arachidonoyl-lysophosphatidylcholine in carotid atheroma plaque from type 2 diabetic patients. Atherosclerosis. 2016;251:339-347. doi:10.1016/j.atherosclerosis.2016.05.004

[16] – Li X, Fang P, Li Y, et al. Mitochondrial Reactive Oxygen Species Mediate Lysophosphatidylcholine-Induced Endothelial Cell Activation. Arterioscler Thromb Vasc Biol. 2016;36(6):1090-1100. doi:10.1161/ATVBAHA.115.306964.

[17] - Chaudhuri P, Rosenbaum MA, Sinharoy P, Damron DS, Birnbaumer L, Graham LM. Membrane translocation of TRPC6 channels and endothelial migration are regulated by calmodulin and PI3 kinase activation. Proc Natl Acad Sci U S A. 2016;113(8):2110-2115. doi:10.1073/pnas.1600371113.

[18] - da Costa RM, da Silva JF, Alves JV, et al. Increased O-GlcNAcylation of Endothelial Nitric Oxide Synthase Compromises the Anti-contractile Properties of Perivascular Adipose Tissue in Metabolic Syndrome. Front Physiol. 2018;9:341. Published 2018 Apr 6. doi:10.3389/fphys.2018.00341.

[19] – Camargo LL, Harvey AP, Rios FJ, et al. Vascular Nox (NADPH Oxidase) Compartmentalization, Protein Hyperoxidation, and Endoplasmic Reticulum Stress Response in Hypertension. Hypertension. 2018;72(1):235-246. doi:10.1161/HYPERTENSIONAHA.118.10824.

[20] - Bánfi B, Tirone F, Durussel I, et al. Mechanism of Ca2+ activation of the NADPH oxidase 5 (NOX5). J Biol Chem. 2004;279(18):18583-18591. doi:10.1074/jbc.M310268200.

[21] - Tostes RC, Wilde DW, Bendhack LM, Webb RC. The effects of cyclopiazonic acid on intracellular Ca2+ in aortic smooth muscle cells from DOCA-hypertensive rats. *Braz J Med Biol Res*. 1997;30(2):257-267. doi:10.1590/s0100-879x1997000200016.

[22] - Ding WX, Ni HM, Gao W, et al. Differential effects of endoplasmic reticulum stress-induced autophagy on cell survival. J Biol Chem. 2007;282(7):4702-4710. doi:10.1074/jbc.M609267200.

[23] - Liu C, Hermann TE. Characterization of ionomycin as a calcium ionophore. J Biol Chem. 1978;253(17):5892-5894.

586 [24] - Kugelmann D, Rotkopf LT, Radeva MY, Garcia-Ponce A, Walter E, Waschke J.
587 Histamine causes endothelial barrier disruption via Ca2+-mediated RhoA activation
588 and tension at adherens junctions. Sci Rep. 2018;8(1):13229. Published 2018 Sep 5.
589 doi:10.1038/s41598-018-31408-3.
590 [25] - Giordano A, Romano S, D'Angelillo A, et al. Tirofiban counteracts endothelial cell
591 apoptosis through the VEGF/VEGFR2/pAkt axis. Vascul Pharmacol. 2016;80:67-74.
592 doi:10.1016/j.vph.2015.12.001.
593 [24] – Lopes RA, Neves KB, Pestana CR, et al. Testosterone induces apoptosis in
594 vascular smooth muscle cells via extrinsic apoptotic pathway with mitochondria-
595 generated reactive oxygen species involvement. *Am J Physiol Heart Circ Physiol*.
596 2014;306(11):H1485-H1494. doi:10.1152/ajpheart.00809.2013.
597 [25] - Dudley SC Jr, Hoch NE, McCann LA, et al. Atrial fibrillation increases production
598 of superoxide by the left atrium and left atrial appendage: role of the NADPH and
599 xanthine oxidases. Circulation. 2005;112(9):1266-1273.
600 doi:10.1161/CIRCULATIONAHA.105.538108.
601 [26] - Dikalov SI, Kirilyuk IA, Voinov M, Grigor'ev IA. EPR detection of cellular and
602 mitochondrial superoxide using cyclic hydroxylamines. Free Radic Res.
603 2011;45(4):417-430. doi:10.3109/10715762.2010.540242.
604 [27] - Neves KB, Nguyen Dinh Cat A, Lopes RA, et al. Chemerin Regulates Crosstalk
605 Between Adipocytes and Vascular Cells Through Nox. Hypertension. 2015;66(3):657-
606 666. doi:10.1161/HYPERTENSIONAHA.115.05616.
607 [28] - Dimitriadis GK, Kaur J, Adya R, et al. Chemerin induces endothelial cell
608 inflammation: activation of nuclear factor-kappa beta and monocyte-endothelial
609 adhesion. Oncotarget. 2018;9(24):16678-16690. Published 2018 Mar 30.
610 doi:10.18632/oncotarget.24659
611 [29] - Kugiyama K, Kerns SA, Morrisett JD, Roberts R, Henry PD. Impairment of
612 endothelium-dependent arterial relaxation by lysolecithin in modified low-density
613 lipoproteins. Nature. 1990;344(6262):160-162. doi:10.1038/344160a0

[30] – Hasegawa H, Lei J, Matsumoto T, Onishi S, Suemori K, Yasukawa M. Lysophosphatidylcholine enhances the suppressive function of human naturally occurring regulatory T cells through TGF-β production. Biochem Biophys Res Commun. 2011;415(3):526-531. doi:10.1016/j.bbrc.2011.10.119

[31] - Chang MC, Lee JJ, Chen YJ, et al. lysophosphatidylcholine induces cytotoxicity/apoptosis and IL-8 production of human endothelial cells: Related mechanisms. Oncotarget. 2017;8(63):106177-106189. Published 2017 Nov 10. doi:10.18632/oncotarget.22425.

[32] - Tsai TY, Leong IL, Cheng KS, et al. Lysophosphatidylcholine-induced cytotoxicity and protection by heparin in mouse brain bEND.3 endothelial cells. *Fundam Clin Pharmacol*. 2019;33(1):52-62. doi:10.1111/fcp.12399.

[33] - Park S, Kim JA, Choi S, Suh SH. Superoxide is a potential culprit of caspase-3 dependent endothelial cell death induced by lysophosphatidylcholine. *J Physiol Pharmacol*. 2010;61(4):375-381.

[34] - Huang YH, Schäfer-Elinder L, Wu R, Claesson HE, Frostegård J. Lysophosphatidylcholine (LPC) induces proinflammatory cytokines by a platelet-activating factor (PAF) receptor-dependent mechanism. Clin Exp Immunol. 1999;116(2):326-331. doi:10.1046/j.1365-2249.1999.00871.x.

[35] - Heinloth A, Heermeier K, Raff U, Wanner C, Galle J. Stimulation of NADPH oxidase by oxidized low-density lipoprotein induces proliferation of human vascular endothelial cells. J Am Soc Nephrol. 2000;11(10):1819-1825.

[36] - Zorov DB, Juhaszova M, Sollott SJ. Mitochondrial reactive oxygen species (ROS) and ROS-induced ROS release. Physiol Rev. 2014;94(3):909-950. doi:10.1152/physrev.00026.2013.

[37] - Egea J, Fabregat I, Frapart YM, et al. European contribution to the study of ROS: A summary of the findings and prospects for the future from the COST action BM1203 (EU-ROS) [published correction appears in Redox Biol. 2018 Apr;14 :694-696]. Redox Biol. 2017;13:94-162. doi:10.1016/j.redox.2017.05.007.

642 [38] - Zorov DB, Juhaszova M, Sollott SJ. Mitochondrial reactive oxygen species (ROS)
643 and ROS-induced ROS release. Physiol Rev. 2014;94(3):909-950.
644 doi:10.1152/physrev.00026.2013.
645 [39] - Giannoni E, Taddei ML, Chiarugi P. Src redox regulation: again in the front line.
646 Free Radic Biol Med. 2010;49(4):516-527. doi:10.1016/j.freeradbiomed.2010.04.025.
647 [40] - Frijhoff J, Dagnell M, Godfrey R, Ostman A. Regulation of protein tyrosine
648 phosphatase oxidation in cell adhesion and migration. Antioxid Redox Signal.
649 2014;20(13):1994-2010. doi:10.1089/ars.2013.5643.
650 [41] - Chen K, Kirber MT, Xiao H, Yang Y, Keaney JF Jr. Regulation of ROS signal
651 transduction by NADPH oxidase 4 localization. J Cell Biol. 2008;181(7):1129-1139.
652 doi:10.1083/jcb.200709049.
653 [42] - Filippini A, D'Amore A, D'Alessio A. Calcium Mobilization in Endothelial Cell
654 Functions. Int J Mol Sci. 2019;20(18):4525. Published 2019 Sep 12.
655 doi:10.3390/ijms20184525.
656 [43] - Chaudhuri P, Colles SM, Damron DS, Graham LM. Lysophosphatidylcholine
657 inhibits endothelial cell migration by increasing intracellular calcium and activating
658 calpain. Arterioscler Thromb Vasc Biol. 2003;23(2):218-223.
659 doi:10.1161/01.atv.0000052673.77316.01.
660 [44] - Murugesan G, Sandhya Rani MR, Gerber CE, et al. lysophosphatidylcholine
661 regulates human microvascular endothelial cell expression of chemokines. J Mol Cell
662 Cardiol. 2003;35(11):1375-1384. doi:10.1016/j.yjmcc.2003.08.004.
663 [45] - Li X, Shao Y, Sha X, et al. IL-35 (Interleukin-35) Suppresses Endothelial Cell
664 Activation by Inhibiting Mitochondrial Reactive Oxygen Species-Mediated Site-Specific
665 Acetylation of H3K14 (Histone 3 Lysine 14). Arterioscler Thromb Vasc Biol.
666 2018;38(3):599-609. doi:10.1161/ATVBAHA.117.310626.
667
668

Supplementary Material and Results

Supplementary figure 1

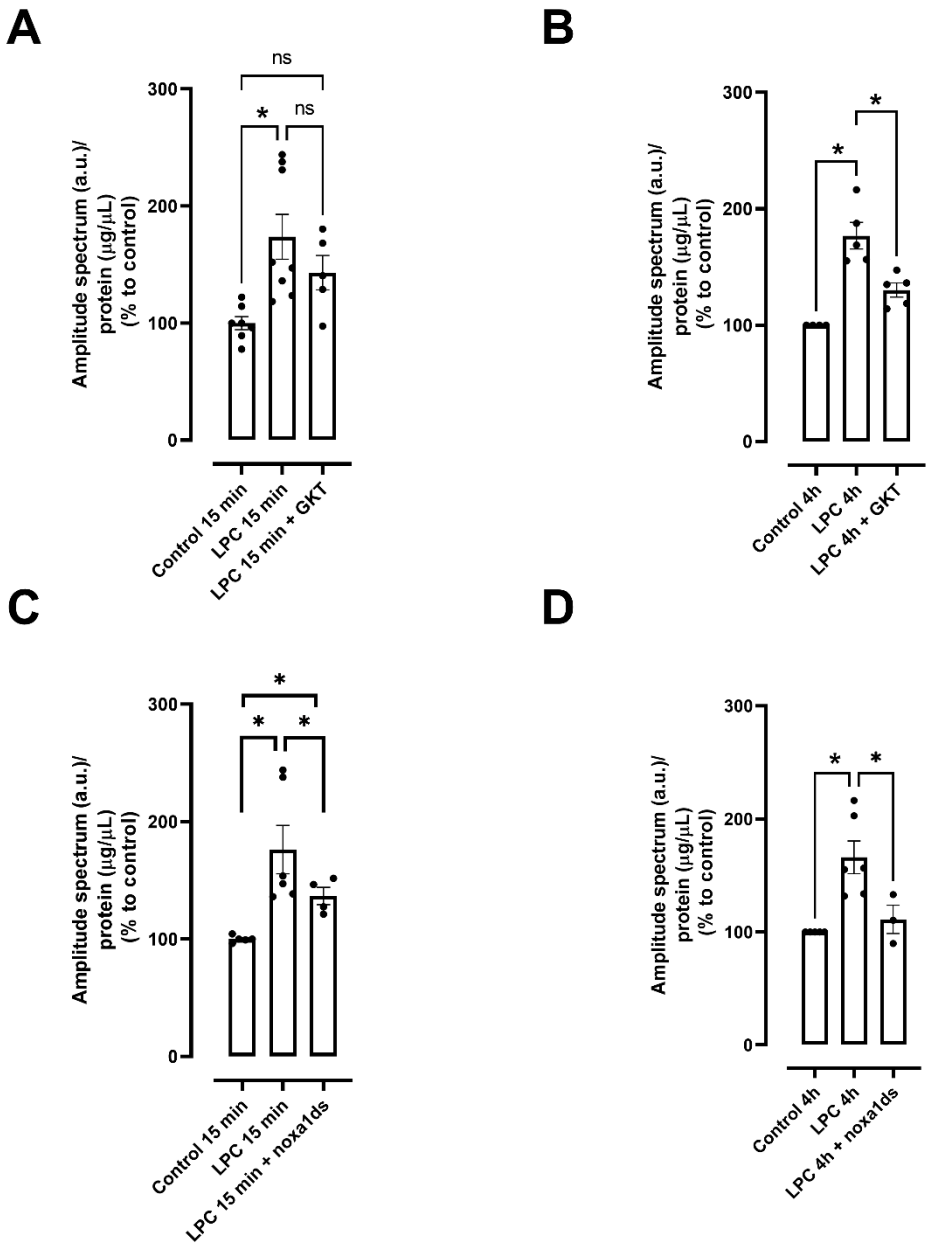

Supplementary Figure 1 - Role of NOX1 and NOX4 in LPC-induced endothelial ROS generation, assessed by EPR spectroscopy. LPC stimulation for 15 min (A, C) and 4 h (B, D) was performed in the presence of vehicle or GKT137831 (10^{-5} M, NOX1/4 inhibitor) or noxa1ds (10^{-5} M, NOX1 inhibitor). Data represent the mean ± SEM of n= 3 – 8 experiments. One-way

677 ANOVA followed by Tukey’s multiple comparisons test. *p<0.05 and, ns= not

678 significant.